ANALYSIS OF SINGLE PARTICLE TRAJECTORIES: FROM NORMAL TO ANOMALOUS DIFFUSION*

R. Metzler, V. Tejedor, J.-H. Jeon

Physics Department, Technical University of Munich
85747 Garching, Germany

Y. He, W.H. Deng, S. Burov, E. Barkai

Department of Physics, Bar Ilan University, Ramat-Gan 52900 Israel

(Received April 2, 2009)

With modern experimental tools it is possible to track the motion of single nanoparticles in real time, even in complex environments such as biological cells. The quest is then to reliably evaluate the time series of individual trajectories. While this is straightforward for particles performing normal Brownian motion, interesting subtleties occur in the case of anomalously diffusing particles: it is no longer granted that the long time average equals the ensemble average. We here discuss for two different models of anomalous diffusion the detailed behaviour of time averaged mean squared displacement and related quantities, and present possible criteria to analyse single particle trajectories. An important finding is that although the time average may suggest normal diffusion the actual process may in fact be subdiffusive.

PACS numbers: 05.40.Fb, 02.50.–r, 87.10.Mn

1. Introduction

The idea to systematically measure individual trajectories of particles in order to obtain information about their ensemble behaviour essentially goes back to Einstein's probabilistic interpretation of diffusion [1]. It was put to much use in the determination of the Avogadro–Loschmidt number in the beginning of the 20th century [2]. In fact single trajectories of small granules in uniform gamboge emulsions obtained by fractional centrifuging were recorded and analysed quantitatively by Jean Perrin in his seminal work on the deduction of Avogadro's constant. A few sample trajectories from Perrin's work are reproduced in Fig. 1.

* Presented at the XXI Marian Smoluchowski Symposium on Statistical Physics Zakopane, Poland, September 13–18, 2008.

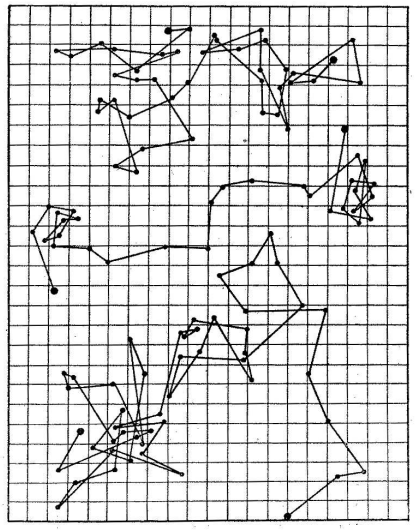

Fig. 1. Three trajectories obtained by tracing a small grain of putty at intervals of 30 sec [3].

It was Nordlund who first devised a setup to obtain long time-resolved trajectory of single particles using a moving photographic film [4]. An example for such a trajectory of a small mercury sphere slowly falling in water is shown in Fig. 2. The Brownian motion superimposed on the drift motion is clearly visible. For each trajectory Nordlund then plotted the mean squared displacement and fitted the diffusion constant. For one single trajectory the result is reproduced in Fig. 3. This is definitely one of the first examples of time averaging in single particle trajectories. In a similar setup with a photographical film Kappler used the stochastic deflection of a small mirror suspended on a long thread to produce single time series of the random torsional movement [5]. This was the last of a long series of experiments to determine Avogadro's number from particle trajectories.

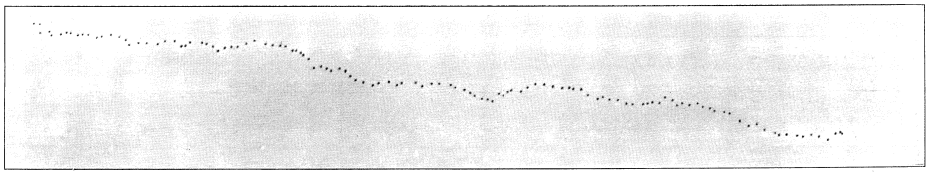

Fig. 2. Stroboscopic trajectory of a small mercury sphere slowly falling in water. The stochastic motion superimposed on the drift produces the wave-like behaviour. Reproduced from [4].

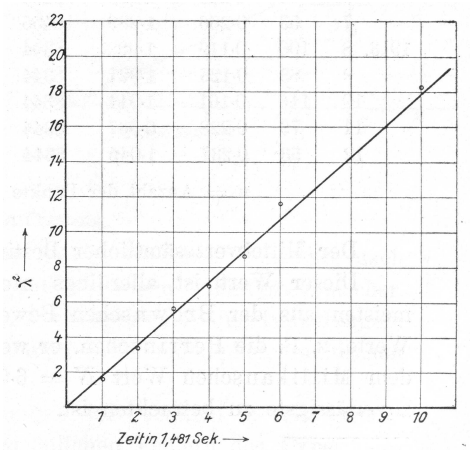

Fig. 3. Mean squared displacement obtained from a single trajectory by Nordlund. The unit of time on the horizontal axis is 1.481 seconds. Nordlund's result for the Avogadro number was remarkable: $5.91{\times}10^{23}$, within 2% of the best current value [4].

In what follows we investigate long time averages for systems that deviate from normal diffusion (Brownian motion), characterised by a linear time dependence of the mean squared displacement. Instead we consider systems displaying subdiffusion of the type

$$\langle x^2(t)\rangle = 2K_\alpha t^\alpha\,, \tag{1}$$

for $0 < \alpha < 1$. Here K_α of dimension $\mathrm{cm}^2/\mathrm{sec}^\alpha$ is the generalised diffusion coefficient. Such anomalous scaling of the mean squared displacement is known from a rich variety of systems including amorphous semiconductors [6], tracer spreading in underground aquifers [7], or diffusion on percolation clusters [8]. Also on smaller scales such subdiffusion has been reported, see the discussion below. Note that equation (1) is an ensemble average,

$$\langle x^2(t)\rangle = \int\limits_{-\infty}^{\infty} x^2 P(x,t)\,dx\,, \tag{2}$$

where $P(x,t)dx$ is the probability to find the particle in the infinitesmial interval $x,\ldots,x+dx$ at time t.

In the following we show that the behaviour of the long time average of the mean squared displacement strongly depends on the actual dynamics underlying the system. In particular we demonstrate that for systems with diverging characteristic waiting times, connected to ageing phenomena, the time-averaged mean squared displacement scales the same way as

for Brownian motion, *i.e.*, the actual subdiffusion cannot be recovered from the time average. Implications of this phenomenon and potential controls when analysing experimental data are discussed.

2. Time averaged mean squared displacement

With modern experimental tools single trajectories of particles down to the nanoscale can be obtained, even in complex systems such as biological cells [9–13]. Often the behaviour of the particles is then inferred from time series analysis. A convenient measure is the time averaged mean squared displacement

$$\overline{\delta^2(\Delta,T)} = \frac{\int_0^{T-\Delta} [x(t'+\Delta)-x(t')]^2 dt'}{T-\Delta}\,. \tag{3}$$

Here T is the overall measurement time, *i.e.*, the length of the obtained time series. Δ, often called the lag time, is the width of the time window sliding across the time series. In an ergodic system the long-time average will provide the same information as the ensemble average.

For a Brownian particle with a typical waiting time τ between successive jumps the number of jumps will on average increase like $\langle n(t)\rangle = t/\tau$. The variance of the step size of each jump on average is $\langle \delta x^2\rangle$. The ensemble average of the quantity (3) will therefore behave like

$$\left\langle \overline{\delta^2(\Delta,T)} \right\rangle = 2K_1\Delta \quad \therefore \quad K_1 \equiv \frac{\langle \delta x^2\rangle}{2\tau}\,, \tag{4}$$

where we defined the diffusion constant K_1. For a Brownian particle we conclude that the time averaged mean squared displacement $\overline{\delta^2}$ is completely equivalent to the ensemble average

$$\langle x^2(t)\rangle = \int_{-\infty}^{\infty} x^2\, P(x,t)dx = 2K_1 t\,, \tag{5}$$

where $P(x,t)dx$ is again the probability to find the particle in the interval $x \ldots x+dx$ at time t. Here we use natural boundary conditions $P(|x|\to\infty,t)=0$ and initial condition $P(x,0)=\delta(x)$. Note that fluctuations around the ensemble average underlying relation (4) will be small for such a Brownian system.

On a finite domain of size L the distance between successive positions of the particle is bounded. Averaging over the equilibrium distribution of variances $[x(t'+\Delta)-x(t')]^2$ in the integral of equation (3) we obtain the quantity $\overline{\delta^2} \sim L^2/12$ ($\Delta \gg L^2/K_1$), the same result as for the ensemble average $\langle x^2\rangle$.

2.1. Experimental evidence

A number of recent experiments report subdiffusion in single tracking experiments. This is particularly important in the current quest to understand transport in biological cells and related processes such as gene regulation. Thus it was shown that adeno-associated viruses of radius $\approx 15\,\mathrm{nm}$ in a cell may perform subdiffusion with $\alpha = 0.5 \ldots 0.9$ [9]; fluorescently labelled messenger RNA chains of length 3000 bases and diameter of some 50 nm subdiffuses with $\alpha \approx 0.75$ [10]; lipid granules of typical size of few hundred nm exhibit $\alpha \approx 0.75 \ldots 0.85$ [11–13]. An analysis imposing normal diffusion on the tracking data of single cell nuclear organelles shows extreme fluctuations as function of time along individual trajectories [14]. These findings are in line with observations from fluorescence correlation spectroscopy for which subdiffusion was observed for membrane protein motion ($\alpha \approx 0.5 \ldots 0.8$) [15] and dextrane polymers of various lengths in living cells and reconstituted crowded environments ($\alpha \approx 0.5 \ldots 1$) [16, 17].

In all these experiments the exact physical nature of the subdiffusion is yet unknown, as well as the time scale over which the subdiffusion persists. Additional information from single particle tracking experiments will be very important to better understand this phenomenon. Below we discuss two important stochastic models for subdiffusion and discuss what other information may be useful.

We note that the nature of subdiffusion is known more precisely from single tracking of submicron plastic beads in a reconstituted actin network of typical mesh size ξ: the subdiffusion was shown to be associated with a power-law waiting time distribution $\psi(\tau) \simeq \tau^{-1-\gamma}$ whose index γ varies between close to zero, for $a/\xi \approx 1$ and larger, up to one for $a/\xi \approx 0.3$, where a is the bead size [18]. For larger particles such as the lipid granules the subdiffusion may therefore be connected to the viscoelasticity of the medium, similar to the *in vitro* experiments of reference [18].

3. Single trajectory analysis for anomalous diffusion

We now return to our analysis of the quantity (3) for subdiffusive processes. We distinguish continuous time random walk subdiffusion and antipersistent fractional Brownian motion.

3.1. Ageing systems

In the continuous time random walk (CTRW) model, originally devised to describe anomalous diffusion of charge carriers in amorphous semiconductors [6], the waiting time τ between successive jumps becomes a random variable. It is distributed with a probability density $\psi(\tau)$. This process can

be interpreted as a particle successively falling into traps [19], whose depth have a certain distribution. If the latter is exponential the distribution of waiting times becomes long-tailed [6, 20]

$$\psi(\tau) \sim \frac{\overline{\tau}^{\alpha}}{|\Gamma(-\alpha)|\tau^{1+\alpha}}, \qquad \tau \to \infty, \tag{6}$$

such that it does not possess a finite characteristic waiting time, a property typical for ageing systems [21]. In equation (6) the correct dimension is ensured by the scale factor $\overline{\tau}$. On an infinite domain the ensemble averaged mean squared displacement takes on the form (1) where the generalised diffusion coefficient is defined through $K_\alpha = \langle \delta x^2 \rangle / [2\Gamma(1+\alpha)\overline{\tau}^{\alpha}]$ [22].

For a system governed by a waiting time distribution of the type (6) the average number of jumps no longer grows linearly in time, but like $\langle n(t) \rangle \sim t^{\alpha}/[\overline{\tau}^{\alpha}\Gamma(1+\alpha)]$. This sublinear growth translates into the mean squared displacement (1), for which one can define an effective time-dependent diffusion constant $\langle x^2(t) \rangle = 2\overline{K}(t)t$ with $\overline{K}(t) = K_\alpha t^{\alpha-1}/\Gamma(1+\alpha)$ that decays over time.

Remarkably the following result is obtained for the time averaged mean squared displacement (3)

$$\left\langle \overline{\delta^2(\Delta, T)} \right\rangle \sim 2K_\alpha \frac{\Delta}{T^{1-\alpha}} = 2\overline{K}(T)\Delta. \tag{7}$$

in the limit $\Delta \ll T$ [23, 24]. As function of the lag time the time averaged mean squared displacement cannot be distinguished from the result (4) for Brownian motion. The linearity in Δ is indeed confirmed from simulations in Fig. 4, in which results for different single trajectories are shown.

A striking feature of Fig. 4 is the scatter between different trajectories as well as deviations from the linear behaviour in some of the trajectories. This randomness of individual trajectories is due to the fact that the underlying waiting time distribution has a diverging characteristic time scale. Similar to the phenomenon of ageing the time average for the individual trajectories is influenced by one or few extremely long waiting times that, due to the scale-freeness, can be of the order of the entire measurement time. This observation holds, no matter how long the observation time T is. In fact for subdiffusive systems of the CTRW type it was shown that ergodicity is no longer fulfilled [25]. As a consequence even a long time average is no longer a fixed quantity but becomes a random variable [26, 27]. For the single trajectory analysis this implies that the time averaged mean squared displacement $\overline{\delta^2}$ is random. Its distribution can be calculated, resulting in the distribution [23]

$$\phi_\alpha(\xi) = \frac{\Gamma(1+\alpha)^{1/\alpha}}{\alpha\xi^{1+1/\alpha}} \, l_\alpha\left(\frac{\Gamma(1+\alpha)^{1/\alpha}}{\xi^{1/\alpha}}\right), \tag{8}$$

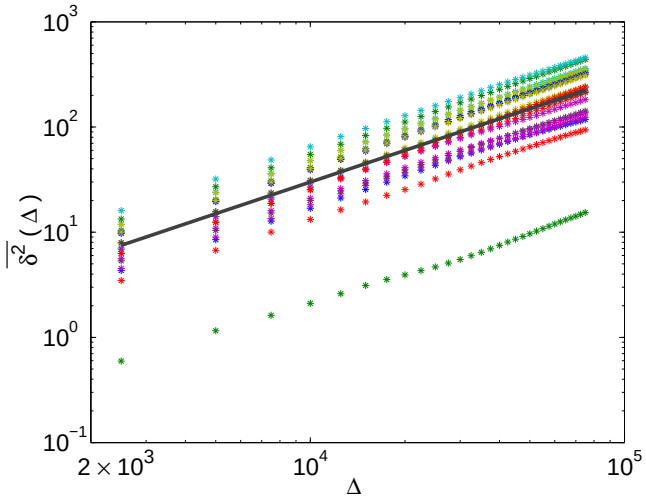

Fig. 4. Simulations of different trajectories of the subdiffusive CTRW process with anomalous diffusion exponent $\alpha = 0.75$ and overall measurement time $T = 10^8$. The dependence of the time averaged mean squared displacement is linear in Δ. A distinct scatter between different, greyscale-coded (colour online) single trajectories is observed. The full line is the average behaviour of the shown trajectories.

valid for long observation times T. In equation (8) we introduce the dimensionless random variable $\xi \equiv \overline{\delta^2}/\langle\overline{\delta^2}\rangle$. Here l_α is a one-sided Lévy stable law whose Laplace image is $\exp(-u^\alpha)$, see reference [23] for details. In the special case $\alpha = 1/2$ the distribution takes on the Gaussian form

$$\phi_{1/2}(\xi) = \frac{2}{\pi}\exp\left(-\frac{\xi^2}{\pi}\right), \tag{9}$$

while in the Brownian limit $\alpha = 1$ we recover the sharp δ result

$$\phi_1(\xi) = \delta(\xi - 1)\,. \tag{10}$$

The latter result is, therefore, equivalent to the known fact that normal Brownian diffusion is ergodic, *i.e.*, the (long) time average is identical to the ensemble average.

For biased diffusion with a constant drift $\langle\delta x\rangle \neq 0$ the time averaged mean displacement

$$\overline{\delta(\Delta, T)} = \frac{\int_0^{T-\Delta}[x(t'+\Delta) - x(t')]dt'}{T-\Delta} \tag{11}$$

is of interest. Indeed, using similar arguments it can be shown that for $\Delta \ll T$ the ensemble average of $\overline{\delta}$ becomes

$$\left\langle \overline{\delta(\Delta, T)} \right\rangle \sim \frac{\langle \delta x \rangle}{\overline{\tau}^{\alpha}\, \Gamma(1+\alpha)} \frac{\Delta}{T^{1-\alpha}}\,, \tag{12}$$

while the distribution of $\xi = \overline{\delta}/\langle \overline{\delta} \rangle$ is again given by equation (8) [23]. Not surprisingly, a similar result has recently been reported for a washboard potential in presence of a drift [28], pointing at the generic character of our result (8). We note that for the constant drift case a generalisation of the Einstein relation of the form $\langle \overline{\delta} \rangle_F = F \langle \overline{\delta^2} \rangle / [2 k_{\mathrm{B}} T]$ is revealed [23], relating the time averages of the first moment under constant bias force F with the time averaged mean squared displacement in absence of the bias.

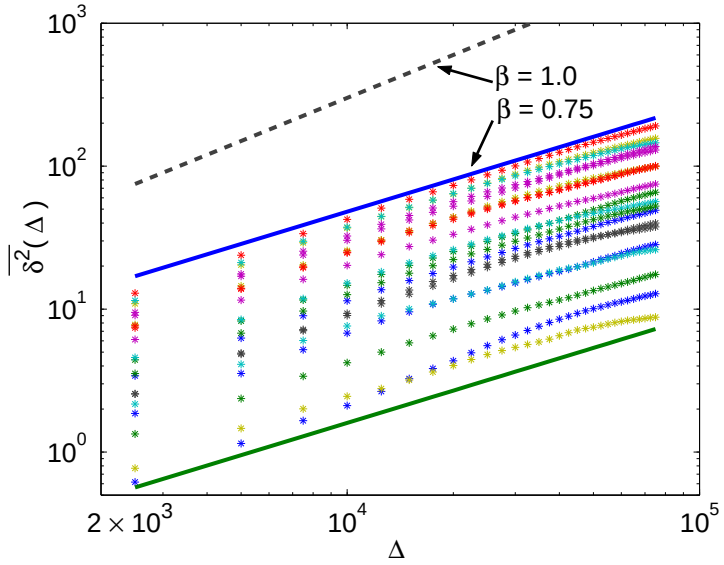

Fig. 5. Time averaged mean squared displacement for a lattice of size 62, for $T = 10^8$ and $\alpha = 3/4$ (colour online). See text.

How does the time averaged mean squared displacement evolve in a finite system? One would expect that for short times the linear growth in Δ should hold while for longer times effects of the boundaries are seen. This is demonstrated in Fig. 5. There the parameters were chosen such that the resulting figure strongly resembles the experimental data from reference [10]. It becomes obvious from the data that the turnover from the proportionality $\sim \Delta$ to a new regime appears like a power-law of slope 0.75. The exact form of the turnover and the behaviour for longer Δ are currently under investigation [29].

In Fig. 6 we show numerical results for the time averaged mean squared displacement as function of Δ on a finite domain. Here, we also include a truncation of the waiting time distribution $\psi(\tau)$ for long τ in the form of a tempered distribution. It is seen that without truncation the quantity $\overline{\delta^2}$ does not reach the stationary value of the ensemble average, but continues to grow. When the truncation is introduced the diffusion eventually turns over to normal diffusion for sufficiently long times (because of the boundaries), and Brownian behaviour is recovered. In particular we see that all curves in Fig. 6 turn over to the constant plateau determined by the interval length.

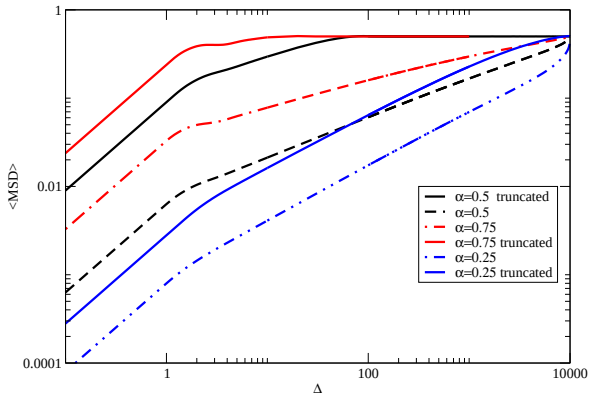

Fig. 6. Time averaged mean squared displacement as function of lag time Δ on a finite domain. The dashed lines are results for the CTRW waiting time distribution $\psi(\tau) \simeq \overline{\tau}^{\alpha}/\tau^{1+\alpha}$ while the full lines include a truncation of the power-law behaviour such that for longer times Brownian behaviour is recovered, and a well-defined plateau value reached. See our forthcoming paper [29] for details.

3.2. Fractional Brownian motion

The CTRW model is widely used to model anomalous diffusion phenomena. However, it is by far not the only stochastic model producing anomalous behaviours of the form (1). We here mention fractional Brownian motion, the famed stochastic process introduced by Mandelbrot and van Ness [31], according to whose definition fractional Brownian motion for a given Hurst parameter $0 < H < 1$ is given by

$$B_{\mathrm{H}}(t) = \frac{1}{\Gamma(H+1/2)} \times \left(\int_0^t (t-\tau)^{H-1/2} dB(\tau) \int_{-\infty}^0 \left[(t-\tau)^{H-1/2} - (-\tau)^{H-1/2} \right] dB(\tau) \right) . \quad (13)$$

Here the integrator B corresponds to ordinary Brownian motion.

Fractional Brownian motion is a self-similar Gaussian process whose increments are stationary [31]. Its covariance follows the form

$$\langle x(t_1)x(t_2)\rangle = D_{\rm H}\Big(t_1^{2H} + t_2^{2H} - |t_1 - t_2|^{2H}\Big)\,, \qquad t_1\,,\ t_2 > 0\,, \tag{14}$$

such that the mean squared displacement is of the form (1) with $\alpha = 2H$ and K_α replaced by $D_{\rm H} = \Gamma(1-2H)\cos(\pi H)/[2\pi H]$. Fractional Brownian motion therefore covers the whole range of anomalous diffusion including subdiffusion $H < 1/2$, normal diffusion $H = 1/2$, superdiffusion ($1/2 < H < 1$) and ballistic motion ($H = 1$). In the latter the particle constantly moves in one given direction. The resulting trajectory of fractional Brownian motion is distinguished by a fractal dimension $d_{\rm f} = 1/H$ [32]. That means that for subdiffusion this process has a trajectory that is more space-filling than both ordinary Brownian motion and CTRW subdiffusion.

Sometimes also different processes are subsumed under the notion of fractional Brownian motion. These are stochastic differential equations with power-law memory kernel (fractional Langevin equations) [33, 34].

Due to its stationarity we would expect fractional Brownian motion to be ergodic in the sense that the long time average and the ensemble mean coincide. Indeed it can be demonstrated that the ensemble average of the time averaged mean squared displacement becomes [33]

$$\left\langle \overline{\delta^2(\Delta, T)} \right\rangle = 2D_{\rm H}\Delta^{2H}\,. \tag{15}$$

Its equivalence $\langle\overline{\delta^2}\rangle = \langle x^2\rangle$ to the ensemble averaged mean squared displacement indeed corroborates ergodicity. However, the analysis in reference [33] shows that *(i)* the convergence to ergodicity is slow and, somewhat surprisingly, *(ii)* the convergence as function of time shows a critical point at $H = 3/4$. More explicitly, defining the normalised variance

$$V = \frac{\left\langle \left(\overline{\delta^2(\Delta, T)}\right)^2 \right\rangle - \left\langle \overline{\delta^2(\Delta, T)} \right\rangle^2}{\left\langle \overline{\delta^2(\Delta, T)} \right\rangle^2}\,, \tag{16}$$

it turns out that [33]

$$V \sim k(H) \begin{cases} \Delta/T\,, & 0 < H < 3/4 \\ \Delta(\log T)/T\,, & H = 3/4 \\ (\Delta/T)^{4-4H}\,, & 3/4 < H < 1 \end{cases}\,. \tag{17}$$

The coefficient $k(H)$ shows a non-smooth transition at $H = 3/4$ with a divergence on reaching $H = 3/4$ both from below and above, as shown in Fig. 7. At $H = 3/4$ the finite value $k(H) = 9/16 = 0.5625$ is found. Finally, we note that in the ballistic limit $H = 1$ ergodicity is broken, as naively expected for a particle that does not change direction.

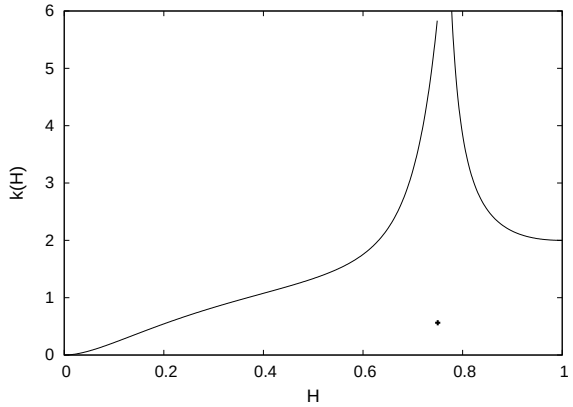

Fig. 7. Behaviour of the prefactor $k(H)$ from equation (17) as function of the Hurst coefficient H. Note the finite value $H = 3/4$.

4. Data analysis

Given actual data in the form of time series from single particle tracking, how can one decide which process is underlying the dynamics? We here list a number of properties that may be investigated.

4.1. Trajectories

The trajectories obviously contain more information than the mean squared displacement. In particular one can measure the waiting time distribution from stalling events in the trajectories. For pronounced subdiffusive processes with power-law waiting time distribution immobilisation events should be observed, *i.e.*, for certain time spans neither coordinate should show significant variation, see, for instance, the trajectories shown in reference [18]. Due to the scale-free nature of CTRW subdiffusion these immobilisations should span multiple time scales. If such events occur they are indicative of the nature of the process. Absence of such features in shorter time series cannot necessarily rule out the CTRW dynamics, in particular for α closer to one very distinct immobilisation are relatively rare events and possibly require long time series.

From the trajectory additional criteria can be inferred. Thus one can check the temporal statistics for a particle coordinate x remaining above or below a certain threshold value x_t. If the process is non-stationary one would expect a weak ergodicity breaking for the long time averaged probability of being above or below x_t, *i.e.*, this time average becomes a random variable.

4.2. Variation of the measurement time

As derived above the time averaged results distinctly depend on the overall measurement time T. Thus CTRW subdiffusion displays an effective diffusion constant entering the time averaged mean squared displacement, see equation (7). This $\overline{K}(T)$ decays with increasing T as a power-law, reflecting the ageing of the system. Fractional Brownian motion's convergence to ergodicity includes a T-dependence in the normalised variance V in equation (17). If it is possible to vary T significantly it could provide very useful information.

4.3. Scatter

Naturally, finite time series for single particle trajectories show scatter. For ergodic processes this scatter will decay as function of the measurement time T, *i.e.*, the longer the time average is running the more the result converges to the ensemble behaviour. The variance of the scatter will tend to vanish over time. In contrast, for a process with diverging time scale the scatter is strong and persists over the entire measurement time T, no matter how long T is chosen (as long as it is shorter than an eventual truncation time of the power-law). As it stands the scatter is possibly one of the most

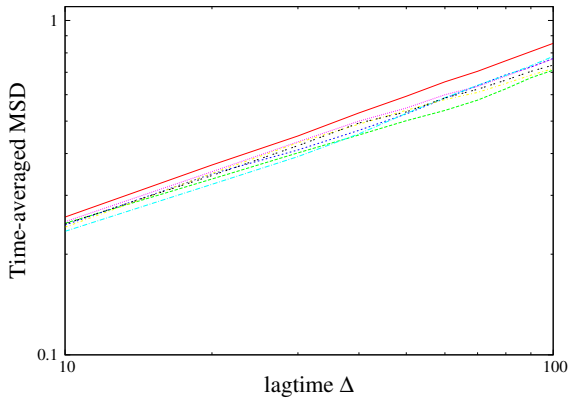

Fig. 8. Simulation of individual trajectories for fractional Brownian motion for an interval of length 10 and Hurst exponent $H = 1/4$. The run time was 4096. Note that the scatter becomes more pronounced with increasing Δ. For longer Δ (not shown here) a plateau is reached, however, closer to T the data become significantly more noisy.

significant parameters available from single particle tracking. Numerical studies suggest that very pronounced scatter would be expected from CTRW subdiffusion while fractional Brownian motion-type dynamics show much less scatter, a typical result is shown in Fig. 8.

Of course, one cannot exclude that (part of) the scatter in the experimental data may be due to spatial inhomogeneities, in particular, in systems as complex as biological cells. Recent studies on lipid granules in living cells suggest that at least the anomalous diffusion exponent is independent of the location of the granule in the cell [13]. However, more experimental data are necessary to tell whether the scatter is predominantly a dynamic feature, or not.

4.4. Ergodicity parameter

A convenient measure for the breaking of ergodicity is the parameter

$$\mathrm{EB} = \lim_{T\to\infty} \frac{\left\langle \left(\overline{\delta^2}\right)^2 \right\rangle - \left\langle \overline{\delta^2} \right\rangle^2}{\langle \overline{\delta^2} \rangle^2} = \frac{2\Gamma(1+\alpha)^2}{\Gamma(1+2\alpha)} - 1\,, \tag{18}$$

where the right hand side holds for the CTRW subdiffusion model. The parameter EB varies from EB = 1 for $\alpha \to 0$ monotonically to EB = 0 for the Brownian limit $\alpha = 1$. In the special case $\alpha = 1/2$ one finds EB = $\pi/2 - 1 \approx 0.57$, while for $\alpha = 0.75$, EB≈ 0.27. Simulations analysis shows that the EB parameter is a reliable parameter, however, convergence may be slow [23].

For fractional Brownian motion the normalised variance V from equation (17) can also be defined as a measure for ergodicity breaking. For finite measurement times its value is non-zero, decaying slowly. Variation of the overall measurement time T may, therefore, decide whether the ergodicity breaking parameter attains the constant value expected for a non-stationary process, or decays to zero as expected for fractional Brownian motion-type processes.

4.5. First passage statistics

Information can also be obtained from the analysis of the first passage behaviour in a particle trace, we refer to the detailed discussion in reference [35].

With sufficiently long time series it is possible to discriminate diffusive mechanisms from the distribution of first passage times, see the discussion in a forthcoming paper [36].

4.6. Maximum statistics

An alternative approach to the single trajectory analysis is to calculate the mean maximal excursion. Is $P_{\rm sup}(x_0,t)$ the probability density that the maximal distance from the starting point reached by the particle from time 0 until t, then we calculate the mean-max variance

$$\mathfrak{m}^2 \equiv \int_0^\infty x_0^2 P_{\rm sup}(x_0,t)dx_0\,. \tag{19}$$

A detailed investigation of this and related quantities will be presented in a forthcoming paper [36]. Preliminary investigations show that the maximum statistics allows better estimates of the dynamic parameters than regular moments.

Another way to examine the data by maximum statistics is to determine the probability that the trajectory within a given time stays within a shell of radius $x_0 t^{\alpha/2}$, that is growing with time. In Fig. 9 we show an analysis of actual experimental data with relatively short trajectories (1000 steps). Averaging over a modest number of trajectories produces a remarkably good data collapse, see reference [36] for details.

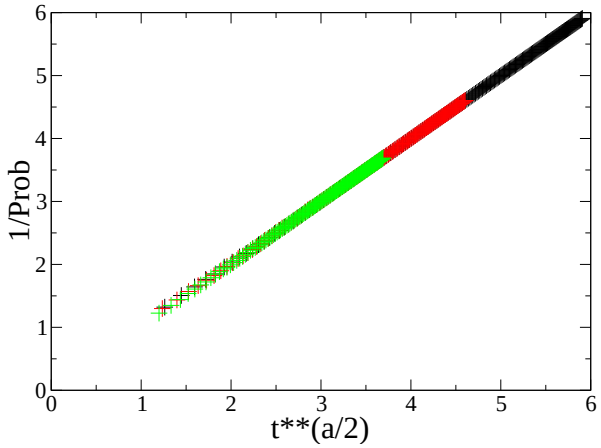

Fig. 9. Plot of one over the probability that the trajectory still is within a shell of growing radius $x_0 t^{\alpha/2}$, as function of scaled time $t^{\alpha/2}$. Data points are from single particle tracking experiments in a crowding agent [36]. The plot shows three subsets with 293, 243 and 234 trajectories, respectively. The longest trajectories have 1000 steps.

5. Conclusions

Single particle tracking is developing towards a standard tool to probe local physical properties of complex systems. As it delivers the complete or, at least, projected trajectory of an individual particle, the information content of the obtained time series is potentially higher than from other experiments such as fluorescence correlation. One challenge is to extract this information, and relate this to the underlying physical mechanisms governing the transport behaviour. This, in turn, requires knowledge on the statistical behaviour connected with given stochastic processes. Here we analysed some important quantities in the continuous time random walk model and for fractional Brownian motion.

For CTRW subdiffusion even a long time average remains a random quantity, no matter how long the measurement time T is chosen. This is intimately connected to the non-stationary behaviour and ageing properties due to the divergence of the characteristic waiting time. We showed that although random the time averaged quantities have a distribution, and can be characterised by certain quantities such as the time averaged mean squared displacement and its scatter, or the ergodicity breaking parameter.

Fractional Brownian motion is stationary and ergodic, its time averages are identical to the ensemble quantities. However, the approach to ergodicity in a given trajectory is slow.

We discussed various options to analyse single particle trajectories. While for sufficiently long time series these quantities should allow one to distinguish between different stochastic mechanisms such as subdiffusion in the CTRW or fractional Brownian motion frameworks, short time series will possibly not allow clearcut statements. Thus, for the example of the data from reference [10] it would be appealing to say that the power-law behaviour is real and due to a fractional Brownian motion-type dynamics instead of a turnover behaviour that only looks like a power-law. However, the significant scatter of the anomalous diffusion constant would rather point towards the CTRW interpretation involving ageing. In similar experiments the variation of the overall measurement time T is desirable to be able to distinguish different mechanisms. These questions are quite fundamental in our understanding of nonequilibrium phenomena in complex systems.

A final comment on the issue of non-stationarity is in order. Systems such as biological cells are changing incessantly. They grow, feed, divide, and in this consume energy provided by food. On a molecular level small molecules such as water or salts are constantly exchanged on the inter and intracellular level, and biopolymers such as proteins, RNA, DNA, or cytoskeletal fibres are constantly being produced or decay. While this allows quick equilibration of, *e.g.*, hydrostatic or osmotic pressure with the envi-

ronment there is no necessity for a cell to be completely stationary. In fact non-stationary behaviour may in some cases even be beneficial.

We thank Joseph Klafter, Michael Lomholt, Friedrich Simmel, Igor Sokolov, and Irwin Zaid for useful discussions. We also acknowledge funding from the Deutsche Forschungsgemeinschaft (DFG). Eli Barkai thanks the Israel Science Foundation for support.

REFERENCES

[1] A. Einstein, *Ann. Phys. (Leipzig)* **17**, 549 (1905); **19**, 371 (1906) see also *Albert Einstein — Investigations on the Theory of the Brownian Movement*, ed. R. Fürth, Dover, New York 1956.

[2] S.E. Virgo, *Sci. Prog.* **27**, 634 (1933).

[3] J. Perrin, *Comptes Rendus (Paris)* **146**, 967 (1908); *Ann. Chim. Phys.* **18**, 5 (1909).

[4] I. Nordlund, *Z. Physik. Chemie* **87**, 40 (1914).

[5] E. Kappler, *Ann. Phys. (Leipzig)* **11**, 233 (1931).

[6] H. Scher, E. Montroll, *Phys. Rev.* **B12**, 2455 (1975).

[7] H. Scher, G. Margolin, R. Metzler, J. Klafter, B. Berkowitz, *Geophys. Res. Lett.* **29**, 1061 (2002).

[8] A. Klemm, R. Metzler, R. Kimmich, *Phys. Rev.* **E65**, 021112 (2002).

[9] G. Seisenberger, M.U. Ried, T. Endress, H. Büning, M. Hallek, C. Bräuchle, *Science* **294**, 1929 (2001).

[10] I. Golding, E.C. Cox, *Phys. Rev. Lett.* **96**, 098102 (2006).

[11] A. Caspi, R. Granek, M. Elbaum, *Phys. Rev. Lett.* **85**, 5655 (2000).

[12] I.M. Tolić-Nørrelykke, E.L. Munteanu, G. Thon, L. Oddershede, K. Berg-Sorensen, *Phys. Rev. Lett.* **93**, 078102 (2004).

[13] C. Selhuber-Unkel, P. Yde, K. Berg-Sørensen, L.B. Oddershede, *Physical Biology*, in press.

[14] M. Platani, I. Goldberg, A.I. Lamond, J.R. Swedlow, *Nat. Cell Biol.* **4**, 502 (2002).

[15] M. Weiss, H. Hashimoto, T. Nilsson, *Biophys. J.* **84**, 4043 (2003).

[16] M. Weiss, M. Elsner, F. Kartberg, T. Nilsson, *Biophys. J.* **87**, 3518 (2004).

[17] D.S. Banks, C. Fradin, *Biophys J.* **89**, 2960 (2005).

[18] I.Y. Wong, M.L. Gardel, D.R. Reichman, E.R. Weeks, M.T. Valentine, A.R. Bausch, D.A. Weitz, *Phys. Rev. Lett.* **92**, 178101 (2004).

[19] R. Metzler, J. Klafter, *J. Phys. Chem.* **B104**, 3851 (2000); *Phys. Rev.* **E61**, 6308 (2000).

[20] S. Burov, E. Barkai, *Phys. Rev. Lett.* **98**, 250601 (2007).

[21] E. Barkai, Y.C. Cheng, *J. Chem. Phys.* **118**, 6167 (2003).

[22] R. Metzler, J. Klafter, *Phys. Rep.* **339**, 1 (2000); E. Barkai, R. Metzler, J. Klafter, *Phys. Rev.* **E61**, 132 (2000).

[23] Y. He, S. Burov, R. Metzler, E. Barkai, *Phys. Rev. Lett.* **101**, 058101 (2008) see also the Viewpoint, I.M. Sokolov, *Physics* **1**, 8 (2008).

[24] A. Lubelski, I.M. Sokolov, J. Klafter, *Phys. Rev. Lett.* **100**, 250602 (2008).

[25] J.-P. Bouchaud, *J. Phys. (Paris)* **2**, 1705 (1992).

[26] A. Rebenshtok, E. Barkai, *J. Stat. Phys.* **133**, 565 (2008); G. Bel, E. Barkai, *Phys. Rev. Lett.* **94**, 240602 (2005).

[27] M.A. Lomholt, I.M. Zaid, R. Metzler, *Phys. Rev. Lett.* **98**, 200603 (2007).

[28] I.M. Sokolov, E. Heinsalu, P. Hänggi, I. Goychuk, `arXiv:0811.4738`.

[29] S. Burov *et al.*, unpublished.

[30] A. Stanislavsky, K. Weron, A. Weron, *Phys. Rev.* **E78**, 051106 (2008).

[31] B.B. Mandelbrot, J.W. van Ness, *SIAM Rev.* **10**, 422 (1968).

[32] J. Feder, *Fractals*, Plenum Press, New York 1988.

[33] W.H. Deng, E. Barkai, *Phys. Rev.* **E79**, 011112 (2009).

[34] E. Lutz, *Phys. Rev.* **E64**, 051106 (2001).

[35] S. Condamin, O. Bénichou, V. Tejedor, R. Voituriez, J. Klafter, *Nature* **450**, 77 (2007); S. Condamin, V. Tejedor, R. Voituriez, O. Bénichou, J. Klafter, *Proc. Natl. Acad. Sci. USA* **105**, 5675 (2008).

[36] V. Tejedor *et al.*, unpublished.